Precession and Decay of μ Leptons in Copper

J. T. Goetz, M. Kennedy, and A. Ueda
University of California Los Angeles
(Dated: May 11, 2004)

The mean lifetime of μ^+ leptons is measured as well as the mean lifetime of μ^- leptons in copper. With a uniform magnetic field inside the copper, the precession rate of the μ^+ particles are measured which allows the value of Dirac's *g-factor* to be calculated experimentally. The mean lifetime of the μ^+ lepton is found to be 2180 ± 27 ns, the μ^- lifetime in copper is found to be 170 ± 16 ns, and the calculated value of g is 2.0 ± 0.1.

PACS numbers: 14.60.Ef, 13.35.Bv

I. INTRODUCTION: COSMIC RAYS TO μ LEPTONS

High energy photons from the interstellar medium are constantly bombarding the Earth. These so called cosmic rays, as well as high energy protons, collide with molecules in the upper atmosphere producing showers of π mesons. These π mesons have a mean lifetime of 2.6×10^{-8} seconds and decay quickly to μ leptons as diagrammed in Fig. 1. Both positive and negative muons are produced which have a mean lifetime of 2.197×10^{-6} seconds[10] in a vacuum. This is long enough so that the relativistic muons are able to travel from the upper atmosphere to sea level before decaying[5]. The principal decay mode for the muon is an electron or positron, a neutrino, and an anti-neutrino[10] as shown in Fig. 2 for a positive muon.

A. μ^- capture in Copper

The μ^- particle has the property that it can be absorbed in a conductive medium. This process is known as *muon capture*[5] and is shown in Fig. 3. Here, the negative muon is trapped by the Coulomb attraction of the proton and the muon begins to orbit the nucleus. However, the mass of the muon is approximately 200 times the electron and therefore the radius of the orbit is much smaller and the muon gets captured by a proton in the nucleus. The weak interaction produces a neutrino and a neutron.

The rate of decay of any particle is the sum of the rates of the different modes available to it. For example, a particle which has three modes of decay R_1, R_2, and R_3, will have a total decay rate given by the following equation.

$$R_{tot} = R_1 + R_2 + R_3 \tag{1}$$

Since the μ^+ is not subject to capture and there are no other significant decay modes, its mean lifetime, which is the inverse of the rate of decay, remains the known value 2197 ns. With the possibility of absorption, the μ^- has two significant decay modes. The mean lifetime of the μ^- is found by

$$R_{\text{total}} = R_{\text{decay}} + R_{\text{absorption}} \tag{2}$$

where $R_{\text{absorption}}$ is the rate of μ^- capture in copper, R_{decay} is the decay rate of μ leptons in a vacuum, and R_{total} is the decay rate of the μ^- in copper. Notice that in Eqn. 2, $R = \frac{1}{\tau}$ where τ is the mean lifetime of a particle with a decay rate of R. Substituting the values of the mean lifetime for the μ leptons, we can solve for the absorption rate.

$$R_{\text{absorption}} = \frac{1}{\tau_{\mu^-}} - \frac{1}{\tau_{\mu^+}} \tag{3}$$

Here, τ_- is the mean lifetime of μ^- in copper and τ_{μ^+} is the mean lifetime of the μ lepton in a vacuum.

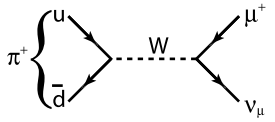

FIG. 1: Feynman diagram of a π^+ decaying via a weak interaction to a μ^+ and a μ-neutrino.

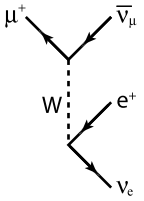

FIG. 2: Feynman diagram of a μ^+ lepton decaying weakly to a positron, electron-neutrino, and an anti-muon-neutrino.

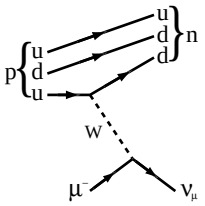

FIG. 3: Feynman diagram of μ^- capture.

B. Precession of μ leptons in magnetic field

The muon has an intrinsic spin $\frac{1}{2}$ which produces a magnetic moment. In a uniform magnetic field, this magnetic moment precesses about the direction of the field. The frequency is given by the following equation:

$$\omega = \frac{geB}{2m_\mu c} \tag{4}$$

In this experiment, we create a uniform magnetic field using a solenoid of copper wiring. The magnetic field is given as:

$$B = \mu_0 n I. \tag{5}$$

To work in *cgs* units, Eqn. 5 can be found in terms of the current through the wires.

$$\begin{aligned} B_{\text{ (gauss)}} = \; & 10^4 \; \tfrac{\text{gauss}}{\text{tesla}} \; 4\pi \times 10^{-7} \; \tfrac{\text{tesla}\cdot\text{m}}{\text{amp}} \\ & \times 695.3 \; \tfrac{\text{turns}}{\text{m}} \; \text{I}_{\text{ (amp)}} \end{aligned} \tag{6}$$

Also, the factor $e/2m_\mu c$ can be expressed as one number with the units of gauss $\times$ sec^{-1}.

$$\begin{aligned} \frac{e}{2m_\mu c} &= \frac{2.55 \times 10^{15} \; \frac{\text{statcoul}}{\text{g}}}{2\left(2.9979 \times 10^{10} \; \frac{\text{cm}}{\text{sec}}\right)} \\ &= 4.253 \times 10^4 \; \tfrac{1}{\text{gauss}\cdot\text{sec}} \end{aligned} \tag{7}$$

If we then set $I = 3.71 \pm 0.01$ amps—which is the current used in this experiment—and solve for g, we get an expression to obtain the *g-factor* from the precession frequency in radians per nanosecond:

$$g = (725 \text{ ns})\,\omega. \tag{8}$$

The current I in Eqn. 6 contains the only significant contribution to the error of the factor 725 in Eqn. 8. The error of this factor is found to be $\approx \frac{1}{2}\%$. We note that the error on ω is approximately 10% while the error in the factor is less than 1% so the factor of 725 is taken without error in Eqn. 8.

II. EXPERIMENT: DESCRIPTION OF APPARATUS

The physical detector as shown in Fig. 4 consists of the following main parts:

- Scintillators and PMTs
- Iron Filter
- Copper Target
- TDC and NIM modules
- Computer and Crate

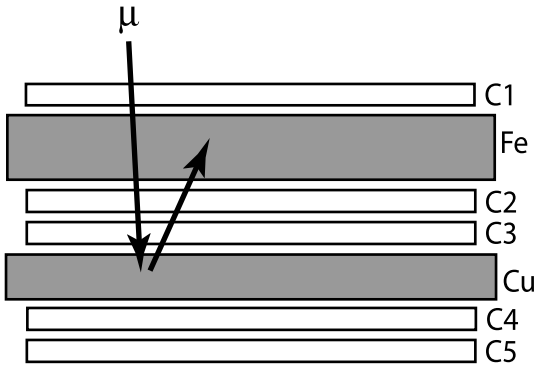

FIG. 4: Physical experimental setup. The scintillators are numbered C1–C5 which are connected to PMTs 1–5 in that order. The start signal is $1 \otimes 2 \otimes 3 \otimes \overline{4}$. The stop signal is $\overline{1}\otimes 2\otimes 3\otimes\overline{4}$ for an upward event and $\overline{1}\otimes\overline{3}\otimes 4\otimes 5$ for a downward event. The iron filter which is $\frac{3}{4}$ inches thick is labeled Fe, and copper target which is $\frac{3}{4}$ inches thick is labeled Cu. An example of an entering muon which subsequently decays to an upward traveling electron is shown.

Each scintillator is connected to a photomultiplier tube (PMT). When a lepton passes through the scintillator, it releases photons which are amplified by a PMT into an electric signal that travels to the discriminators where it is appropriately handled by the logic as seen in Fig. 6. The iron filter has been chosen of a density and thickness such that a muon must have a momentum of at least 240 MeV/c in order to pass through the filter toward the copper target. The copper target has also been carefully chosen to have a density and thickness such that muons with momentum greater than 270 MeV/c will pass straight through and not be stopped by the target. Therefore, each muon absorbed by the copper target must have momentum[9]:

$$240\text{MeV/c} \leq \text{p}_\mu \leq 270\text{MeV/c} \tag{9}$$

A. Testing and adjusting the PMTs

When applying voltage to the PMTs, in this case at approximately -1.2 kV to -1.6 kV, spontaneous discharges will sporadically occur and will show up as signals in discriminator A. The more negative we set the high voltage setting on a PMT, the greater the magnitude of the gain of that PMT. A larger PMT voltage setting corresponds to a larger signal being sent to discriminator A when a muon passes through the scintillator. We do not want to set the PMT voltages too high however, because this increases the likelihood that a series of spontaneous discharges arriving at discriminator A will be mistaken for a muon. For each tube, we take a series of data and plot it as shown in Fig. 5. For the fifth PMT in Fig. 5, we want the efficiency $\frac{2\otimes 3\otimes 5}{2\otimes 3}$ as high as possible without raising the voltage setting as to generate an unreasonably high level of noise. For this PMT, we chose a voltage setting

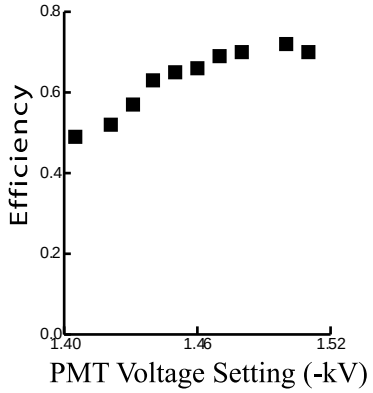

FIG. 5: Efficiency of $\frac{2\otimes3\otimes5}{2\otimes3}$ vs. voltage setting which corresponds to the fifth PMT.

TABLE I: Data for plateau histogram in Fig. 5.

PMT setting (-kV)	$2\otimes3\otimes5$	$2\otimes3$	$\frac{2\otimes3\otimes5}{2\otimes3}$
1.405	488	1005	0.49
1.421	515	998	0.52
1.431	573	1003	0.57
1.440	630	1003	0.63
1.450	652	1001	0.65
1.460	662	998	0.66
1.470	693	1006	0.69
1.480	701	998	0.70
1.500	718	998	0.72
1.510	703	1000	0.70

of -1.48 kV. Similar plots for the other four PMTs may be found in our lab notebook held in the 180F laboratory file cabinet. The settings for all five tubes are shown in Tab. II. PMTs 2, 3 and 4 were each plateaued with $\frac{1\otimes2\otimes3}{1\otimes3}$, $\frac{1\otimes3\otimes4}{1\otimes4}$, and $\frac{1\otimes3\otimes4}{1\otimes3}$ against the voltage settings respectively, yielding efficiencies of at least 90 percent. PMTs 1 and 5 had lower efficiencies because we plateaued them relative to PMTs 2, 3, and 4. However, PMTs 2, 3, and 4 are the most critical in this experiment because they are most used by the TDC stop signals and therefore deserve the highest efficiency. It is difficult to get all five PMTs simultaneously plateaued to the highest possible efficiencies in a short time because each efficiency depends on the voltage settings of each other PMT. To this extent, we saved a great deal of time by setting the most critical PMTs first to high efficiencies while sacrificing some efficiency on the less critical PMTs.

TABLE II: Voltage settings for all 5 PMTs.

PMT	Threshold (-kV)
1	1.46
2	1.40
3	1.40
4	1.40
5	1.48

TABLE III: Threshold settings for the LRS 4608 discriminators in the first stage, A, and the second, B.

Threshold settings		
PMT No.	Discr A	Discr B
C1	-0.037	-0.099
C2	-0.038	-0.117
C3	-0.039	-0.097
C4	-0.040	-0.099
C5	-0.037	-0.097

B. Logic setup for μ lepton decay

The information collected by the PMTs must be rerouted to the correct inputs of the TDC by the logic setup[1] as depicted in Fig. 6. The logic setup consists of the following components:

- 10 Discriminators
- 5 Coincidence Units (AND gates)
- 2 Gate Generators
- 27 LEMO Cables of various lengths

The initial signals sent by the 5 PMTs are sent to the first set of 5 discriminators where they signal are converted to 60 ns NIM signals of amplitude -0.7 V. The second set of 5 discriminators convert the received 60 ns signals to 15 ns signals.

The next stage in our logic is a set of 3 coincidence units. The first coincidence unit has inputs $1\otimes2\otimes3\otimes\overline{4}$. This unit starts the TDC and the two gate generators. The second coincidence unit has inputs $\overline{1}\otimes2\otimes3\otimes\overline{4}$ and sends a stop signal to the TDC's first channel to indicate an upward decay. The third unit has inputs $\overline{1}\otimes\overline{3}\otimes4\otimes5$ and sends a stop signal to the TDC's second channel to indicate a downward decay. Signals of different widths enter these three coincidence units. The veto inputs are of 60 ns width and the signals from discriminator B are of 15 ns width. We adjusted the lengths of the LEMO cables carrying 15 ns signals out of discriminator B to delay them such that they were centered about the 60 ns signals coming out of discriminator A. Fig. 7 depicts what we see on the oscilloscope while looking at the inputs to the decay up coincidence module when we adjust the timing in the lab.

The fourth stage is a set of two gate generators. When a signal is received at this step, the receiving module generates a 20 μs signal. The fifth stage consists of two AND gates which require that the stop signals coming from the 3rd coincidence units are only sent to the TDC if the gate signal from module 4 is open.

C. Data acquisition

The logic routes the signals from the PMTs appropriately so that decay up and decay down events are cor-

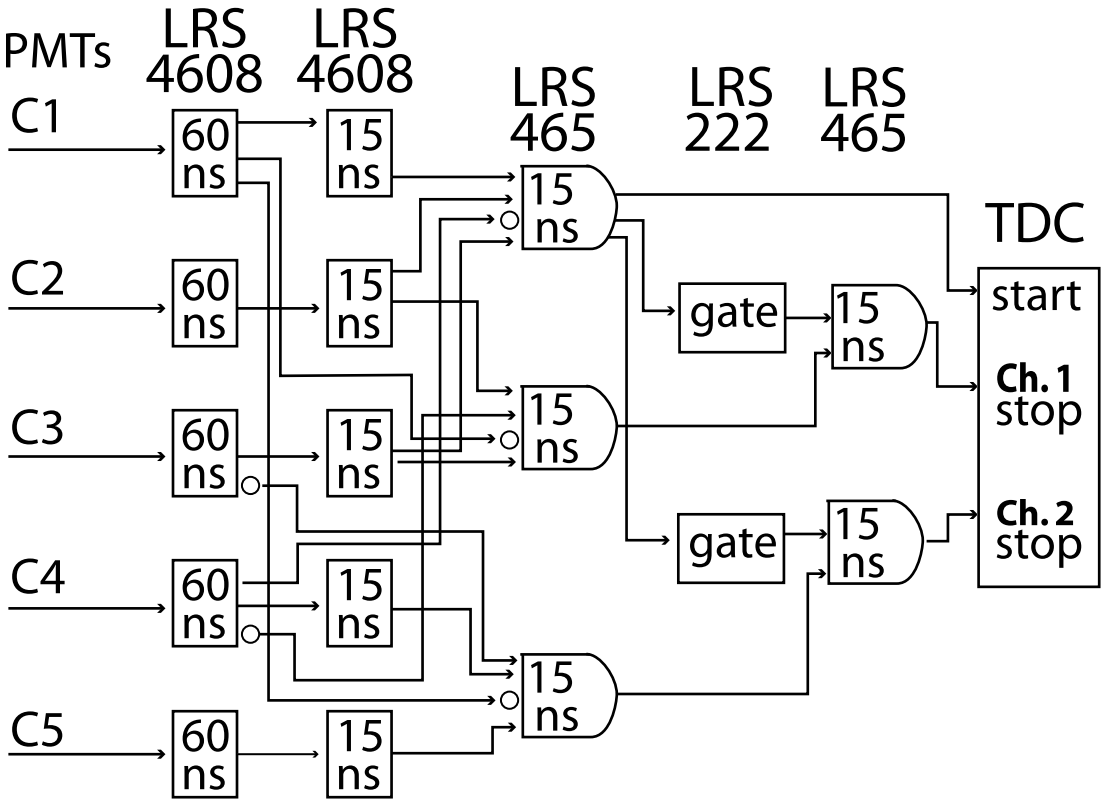

FIG. 6: Logic setup from the inputs of the first discriminators to the TDC. Chanel one corresponds to upward events and channel 2 corresponds to downward events.

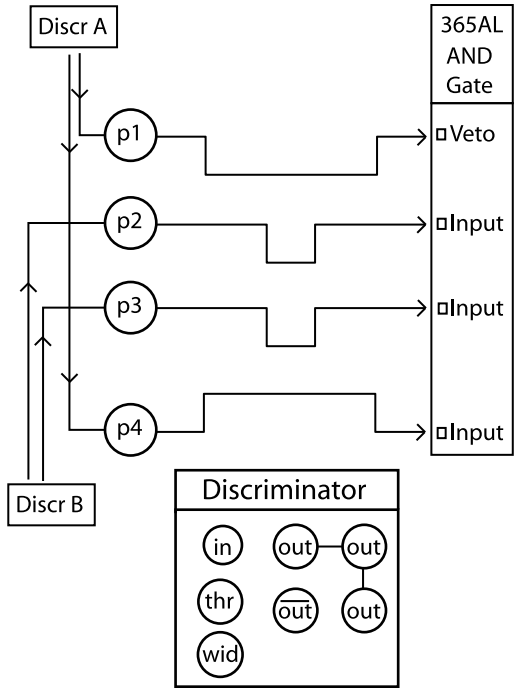

FIG. 7: Input signals to the decay down coincidence unit in the third stage of our logic as seen in Fig. 6. The signal width for Discr A is 60 ns while that for B is 15 ns. A diagram of the discriminator unit is shown below.

rectly timed by the TDC. The information collected by the TDC, however, must still be input to a computer for numerical analysis. This is done via the crate and the CAMAC controller as seen in Fig. 8. There are two parts to the CAMAC. The Crate *Controller* is plugged into the crate where it receives raw data from the TDC through the crate. The second part of the CAMAC is the *interpretor*. The *interpretor* consists of a card that fits into an ISA (Industry Standard Architecture) 16-bit slot of a standard IBM-compatible computer. Accompanying this card is a driver from the manufacturer of the card along with a set of functions that can be used by a computer programmer to read data from the CAMAC *controller*. This *interpretor* is connected to the controller via a parallel in-line communication cable.

1. *BASIC acquisition program*

The Computer receives data from the TDCs through the interpretor of the CAMAC controller. We updated a previously written[3] BASIC data acquisition program. The skeleton of this program is shown below. In this program the variables `D%(1)` and `D%(2)` correspond to data read from the first and second channels in our 8 channel TDC module. The TDC counts every 20 ns: this is the *bin size*. In our set up, `D%(1)` corresponds to

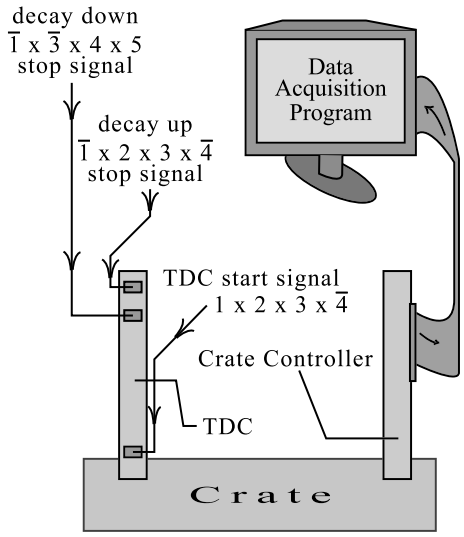

FIG. 8: Data Acquisition

the number of bins counted before the decay up signal stopped the TDC. Thus

$$\text{time(decay up event)} = 20 \times \texttt{D\%(1)} \text{ ns} \qquad (10)$$

The 3rd argument to the function `CAMI` seen in the skeleton of our DAQ program is the number (1–8) of the TDC in the module from which you want to read data. An entry of zero checks to see if there are any -1 entries in the vector whose 8 components each hold the bin counts for one of the TDCs [4]. We cut in the program all data of greater than 2048 bins before it is even written to a file because when we analyze the data, our fit will never need to go beyond 20,000 ns.

```
'**Begin DAQ Main Loop**********************
PRINT "KEY F1 WILL INTERRUPT DAQ"
510 ON KEY(1) GOSUB 150
  KEY(1) ON
  CALL CAMI(S%,8,0,DT%(0),Q%,X%)
'**Check LAM signal from crate
  IF Q% = 0 THEN 510
  GOSUB 4100:  'Read data
'**Drop event if D%(1) or D%(2) overflow
  if D%(1)<0 and D%(2)<0 GOTO 510
  GOSUB 4000:  'Print event to screen
  GOSUB 4200:  'Print event to file
  GOTO 510
900 END

'**Read Ch1 and 2 data from TDC***************
4100 FOR I = 1 TO 2
  A% = I - 1
  IF A% < 1 THEN 4102
'**Calls the CAMI function to retrieve data
'**from the crate modules
  CALL CAMI(S%,2,A%,DT%(0),Q%,X%)
  GOTO 4105
'**Calls the CAMI function to initialize
'**data transfer from the crate modules
4102 CALL CAMI(S%,0,A%,DT%(0),Q%,X%)
'**If event did not time out - record it
4105 IF DT%(0) << 2048 THEN 4108
  D%(I) = -1
  GOTO 4109
'**normalize bin number to time (nanosec)
4108 D%(I) = DT%(0)*20
'**increment the number of either up
'**or down events
  IF D%(1) > 0 THEN
    up% = up% + 1
  ELSE
    down% = down% + 1
  END IF
4109 NEXT I
RETURN
```

D. Measuring $t = t_0$

Referring to our logic diagram in Fig. 6 we see that the start signal travels to the TDC directly from the first AND gate of the third stage. But the stop signals must each travel through a gate generator and and additional coincidence unit before reaching the TDC. There is an inherent delay that the stop signal encounters before reaching the TDC and this delay measured as $t = t_0$ and accounted for in each measurement of our analysis.

To do this we change the start signal from $1 \otimes 2 \otimes 3 \otimes \overline{4}$ to $1 \otimes 3 \otimes 5$. This will now start the TDC for a muon of momentum $p \geq 270$ MeV/c that travels straight through the copper target without being absorbed. The benefit of this is that a "straight through" muon will also trigger both of the TDC stop signals from the second two coincidence units in step 3. The start and stop signals leave step 3 *at the same time*. We would have expected to measure $t = 0$ for each straight through event if there was no delay between the start and stop signals. However, we find a non-zero measurement as anticipated. We want this measurement to be in the center of a bin. We adjusted the lengths of our LEMO cables between steps 4 and 5 so that our t_0 would be as close as possible to 30.0 ns, which is exactly in the center of the second bin.

After taking data under these conditions for 7 minutes and 46 seconds, we accumulated 1412 up hits and 1389 down straight-through hits. We observed that these hits fell into one of the first three 20 nanosecond bins, which run from 0-20, 20-40, and 40-60 nanoseconds. When plotted into a histogram, with the bins on the x-axis and the number of counts on the y-axis, as shown in Fig. 9, we saw that the distributions for up and down hits were both heavily centered about the second bin. This histogram was fitted with a Gaussian curve, and the mean

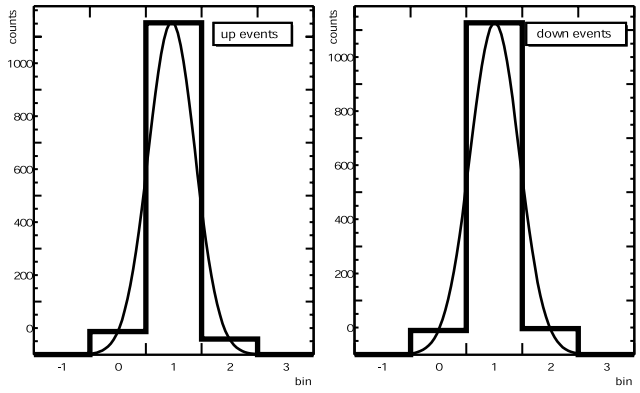

FIG. 9: Zero timing histogram of $1 \otimes 3 \otimes 5$ on the first and second channels of the TDC, which correspond to up and down events respectively. The Gaussian fit facilitates a measurement of the error in any measurement of time in our experiment. This is done by setting σ_t to the standard deviation of the fit.

was found to be:

$$t_0 = 30 \pm 9 \text{ ns} \tag{11}$$

The error propagation involving statistical errors in the mean and sigma as given by ROOT was dominated by the $\sigma = 9$ term. Thus we concluded that the times of each data entry in the rest of our experiment must have 30 ns subtracted from them in order to correct for the delay in the path taken by the TDC stop signals. Also, the timing values produced by the fits must have an error correction due to the σ_t as discussed in Sec. III D.

E. Measuring noise

In order to procure some type of understanding concerning the amount of background we were accumulating in our runs, we performed a series of target out runs, in which the target was swung out of the apparatus and no changes were made to our original logic. There are two types of noise associated with our results:

i After registering a stopping muon signal, a charged particle may conceivably approach the detection apparatus at an extremely oblique angle, hitting $2 \otimes 3$ or $4 \otimes 5$ only. These types of hits would be falsely logged as up or down decays, respectively. Since there is no correlation between any of the events that contribute to this false entry, we would expect this to be a flat distribution of noise, necessitating an added constant in our fitting equation.

ii On occasion, it is possible for a μ-particle to stop in scintillator 3, and cause a start signal, because it is still consistent with our $1 \otimes 2 \otimes 3 \otimes \overline{4}$ trigger. Upon its decay, it will register as an up or down hit. We would expect this type of event to necessitate an exponential term in our fitting equation, since it is in fact a representation of μ-lifetimes.

There is a third type of noise possible, in which a muon stops so close to the surface of scintillator 4 as to not generate a signal, and upon its downward decay, it creates a down stopping signature. As discovered in a Monte Carlo Simulation[2], the occurrence of such events is rare enough as to dismiss their contributions to our histograms.

Here, it is important to note that although both the up and down target-out runs will display a superposition of exponential decay and a flat distribution of noise, when the target is in, all downward propagating μ decays from scintillator 3 will be stopped in the copper target. Therefore, the down target-out data is irrelevant to the rest of our results.

F. μ lepton precession in a magnetic field

Turning on the current in the coils surrounding the copper target, a uniform B-field will run through the target parallel to its axis. The current was chosen to be 3.71 ± 0.01 Amperes. Using the standard formula for the magnetic field in a solenoid as given in Eqn. 5 we find that the magnetic field in the solenoid is approximately 32.4 ± 0.1 Gauss. We kept a cooling fan on the copper coils whenever current was running through them. This keeps the temperature of the coils, and therefore their resistance, approximately constant. Using the formula for the Larmor precession of a muon in a constant magnetic field as given in Eqn. 4, and setting $g = 2$, we should expect a precession rate of 0.000276 radians per nanosecond.

III. ANALYSIS TECHNIQUES

To analyze the data and obtain values for the mean lifetimes of the μ leptons as well as Dirac's *g-factor*, a series of exponential fits were applied to a number of histograms. In particular, the method starts with a zero-timing determination. Then, for the target-in runs, the measured noise was taken into account before being fitted with the appropriate equation. Finally, the target-in data with the magnetic field on is analyzed via a sinusoidal function which produces the rate of precession.

A. Adjusting for noise

In order to adjust for noise as described in Sec. II E, we fit our target out data to Eqn. 12 as seen in Fig. 10 and Tbl. IV.

$$f(t) = A' \exp\left(\frac{-t}{\tau_{\text{noise}}}\right) + B' \exp\left(\frac{-t}{\tau_{\mu^+}}\right) + C' \tag{12}$$

TABLE IV: Ranges of parameters in target out data analysis fit as seen in Eqn. 12 to give Eqn. 22. Each term was fit from $t_{\min}$ to $t_{\max}$ using ROOT. Then, the whole equation was fit over the entire range, [100, 20000], and was fixed or was allowed to vary.

Variable	$t_{\min}$	$t_{\max}$	[100, 20000] fit	Value
A'	100	20000	variable	76 ± 2
τ_{noise}	100	20000	variable	1700 ± 200
B'	100	20000	variable	265 ± 6
τ_{μ^+}	100	20000	fixed	2197
C'	13000	20000	fixed	9.8 ± 0.4

Fixing τ_{μ^+}, which is the mean lifetime of the μ lepton in a vacuum, we let Root's MINUIT analysis program fit the remaining variables so as to get values for τ_{noise} and A'.

B. Fitting μ^+ and μ^- decays

The histogram for μ lepton decay shown in Fig. 11 was fitted with the sum of three exponentials and a constant, corresponding to μ^+ lifetime in copper, τ_{noise}, μ^- lifetime in copper, and a flat distribution of noise throughout.

$$\begin{aligned} f(t) &= A \exp\left(\frac{-t}{\tau_{\mu^-}}\right) \\ &+ B \exp\left(\frac{-t}{\tau_{\mu^+}}\right) \\ &+ C \exp\left(\frac{-t}{\tau_{\text{noise}}}\right) + D \end{aligned} \tag{13}$$

In order to minimize χ^2, and to fit over ranges appropriate to which each term corresponds, the first term of the above function was fitted on the range $t \in [100, 600]$, the second on $t \in [100, 5000]$, the fourth throughout $t \in [100, 20000]$, the and the constant over $t \in [15000, 20000]$. Refer to Tab. V for further clarification.

TABLE V: Ranges of parameters in target-in data analysis fit as seen in Eqn. 13 to give Eqn. 23. Each was term fit from $t_{\min}$ to $t_{\max}$ using ROOT. Then, the whole equation was fit over the entire range, [100, 20000], and was fixed or was allowed to vary.

term	t_{min}	t_{max}	[100, 20000] fit	value
A	100	4000	variable	626 ± 1
τ_{μ^-}	100	4000	variable	170 ± 13
B	100	4000	variable	273 ± 1
τ_{μ^+}	100	4000	variable	2180 ± 25
C	100	20000	fixed	144 ± 3
τ_{noise}	100	20000	fixed	1700 ± 200
D	13000	20000	fixed	6.3 ± 0.1

Here, τ_{noise} is fixed from Eqn. 12. C is found from from normalizing A' from Eqn. 12 by using the ratio of the total run times of the two data sets in the following equation.

$$C = \left(A' \frac{t_{\text{in, up}}}{t_{\text{out, up}}}\right) \tag{14}$$

C. Fitting precession data

In the note by Ticho[9], he explains that the expected decay time histogram, with the magnetic field on, will have two different curves for up and down events. They are given in functional form as follows.

$$\begin{aligned} N_{\text{up}}(t) &= [E + F\cos(\omega t)]\, e^{\frac{-t}{\tau}} \\ N_{\text{down}}(t) &= [E - F\cos(\omega t)]\, e^{\frac{-t}{\tau}} \end{aligned} \tag{15}$$

$$\tag{16}$$

Taking the difference of these will necessarily increase the amplitude of the sinusoidal component, giving

$$N_{\text{up}}(t) - N_{\text{down}}(t) = [G + H\cos(\omega t)]\, e^{\frac{-t}{\tau}}. \tag{17}$$

The range with which to fit this function starts at $t = 800$ ns so as to avoid the times less than about 500 ns where the μ^- decay is dominant. For the end of the range, we chose 10,000 ns because it minimized χ^2 and because the sinusoidal characteristic of the plot was still apparent on this range of $t \in [800, 10000]$.

D. Errors

The errors produced by ROOT's MINUIT analysis program are purely statistical in nature. They are the largest contributer of error to the data. The next significant error in all fits of the histograms is due to the fluctuation of the $t = t_0$ timing. This second error, taken as the σ_t of the Gaussian fit seen in Fig. 9 and Eqn. 11, combines with all errors by the relation below:

$$\sigma_{\text{tot}} = \sqrt{\sigma_t^2 + \sigma_s^2} \tag{18}$$

where σ_s is the statistical error of the values obtained from the fit. For all calculations, $\sigma_t = 9$ so the equation becomes:

$$\sigma_{\text{tot}} = \sqrt{81 + \sigma_s^2}. \tag{19}$$

For the error of the *g-factor*, the percent errors must be used. The formula is as follows.

$$\delta_g = \frac{\delta_\omega}{\omega} g \tag{20}$$

inserting Eqn. 8 into the above equation yields:

$$\delta_g = \frac{\delta_\omega}{\omega} (725 \text{ ns})\, \omega. \tag{21}$$

IV. DATA AND NUMERICAL FITS

In the following formulae, all numbers that do not have errors are fixed before fitting to their perspective histograms. The errors given in these formulae are always statistical, whereas the errors of individual parameters are found from from Eqn. 18.

Data acquisition without the copper target was run for 71.1 hours. Fitting the variables over the appropriate ranges as shown in Tbl. IV resulted in the following:

$$\begin{aligned} f(t) &= (76 \pm 2) \exp\left(\frac{-t}{1700 \pm 200}\right) \\ &+ (265 \pm 6) \exp\left(\frac{-t}{2197}\right) \\ &+ 9.8 \pm 0.4 \end{aligned} \tag{22}$$

Data acquisition with the copper target in and the magnet off was run over a cumulative course of 14 days, 8 hours, 3 minutes, and 43 seconds. We took the data, corrected for $t = t_0$, and binned it into 100ns bins. We fit the data to Eqn. 13 as seen in Fig. 11, which gave:

$$\begin{aligned} f(t) &= (626 \pm 1) \exp\left(\frac{-t}{170 \pm 13}\right) \\ &+ (273 \pm 1) \exp\left(\frac{-t}{2180 \pm 25}\right) \\ &+ (144 \pm 3) \exp\left(\frac{-t}{1700 \pm 200}\right) \\ &+ 6.3 \pm 0.1. \end{aligned} \tag{23}$$

With the magnetic field on, the fit gave:

$$\begin{aligned} N_{\text{up}}(t) - N_{\text{down}}(t) &= (220 \pm 34) + (58 \pm 30) \\ &\times \cos\left((0.00276 \pm 0.00014)\, t\right) \\ &\times \exp\left(\frac{-t}{2100 \pm 180}\right) \\ &+ 0.59 \pm 0.01 \end{aligned} \tag{24}$$

Notice the large error on all but the precession frequency, which is what we are after. This effect is understandable as we did subtract two histograms. This inherently increases the errors of coefficients but has only a small effect on errors inside a functional construct such as a cosine.

V. CONCLUSION

The results show that the μ^+ mean lifetime is

$$\tau_{\mu^+} = 2180 \pm 27 \text{ ns}, \tag{25}$$

the mean lifetime of the μ^- lepton in copper is

$$\tau_{\mu^- \text{ in Cu}} = 170 \pm 16 \text{ ns}, \tag{26}$$

and the precession frequency of the μ lepton in a uniform magnetic field of magnitude 32.4 gauss is

$$\omega = 0.00276 \pm 0.00014 \text{ ns}^{-1}. \tag{27}$$

This gives the value of Dirac's *g-factor*:

$$g = 2.0 \pm 0.1. \tag{28}$$

All of these values agree with the currently accepted values shown here[10]:

$$\begin{aligned} \tau_{\mu^+} &= 2197 \text{ ns} \\ \tau_{\mu^- \text{ in Cu}} &= 164 \pm 2 \text{ ns} \\ g &= 2.00233 \text{ for a muon} \end{aligned} \tag{29}$$

[1] W. E. Slater, *Laboratory Manual for Physics 180F*, UCLA (2002), version 2.1.

[2] W. E. Slater, *Laboratory Manual for Physics 180F*, UCLA (2000), version 2.0.

[3] Y. Shi, *8chtdc.bas*, UCLA (1987).

[4] *Technical Raference Manual: MODEL 6001/6002 CAMAC Controller*, DSP Technology Inc. (1990).

[5] D. Griffiths, *Introduction to Elementary Particles* (John Wiley & Sons, Inc., New York, 1987).

[6] D. H. Perkins, *Introduction to High energy Physics* (Cambridge University Press, Cambridge, 2000), 4th ed.

[7] L. Lyons, *Statistics for Nuclear and Particle Physicists* (Cambridge University Press, Cambridge, 1986).

[8] P. R. Bevington and D. K. Robinson, *Data Reduction and Error Analysis for the Physical Sciences* (McGraw-Hill, Boston, 1992), 2nd ed.

[9] H. Ticho, *180F Experiment: Muon Mean Life and Magnetic Moment*, UCLA High Energy Group (1973).

[10] K. Hagiwara et al., Physical Review **D 66** (2002).

[11] W. R. Smythe, *Static and Dynamic Electricity* (McGraw-Hill, New York, 1968), 3rd ed.

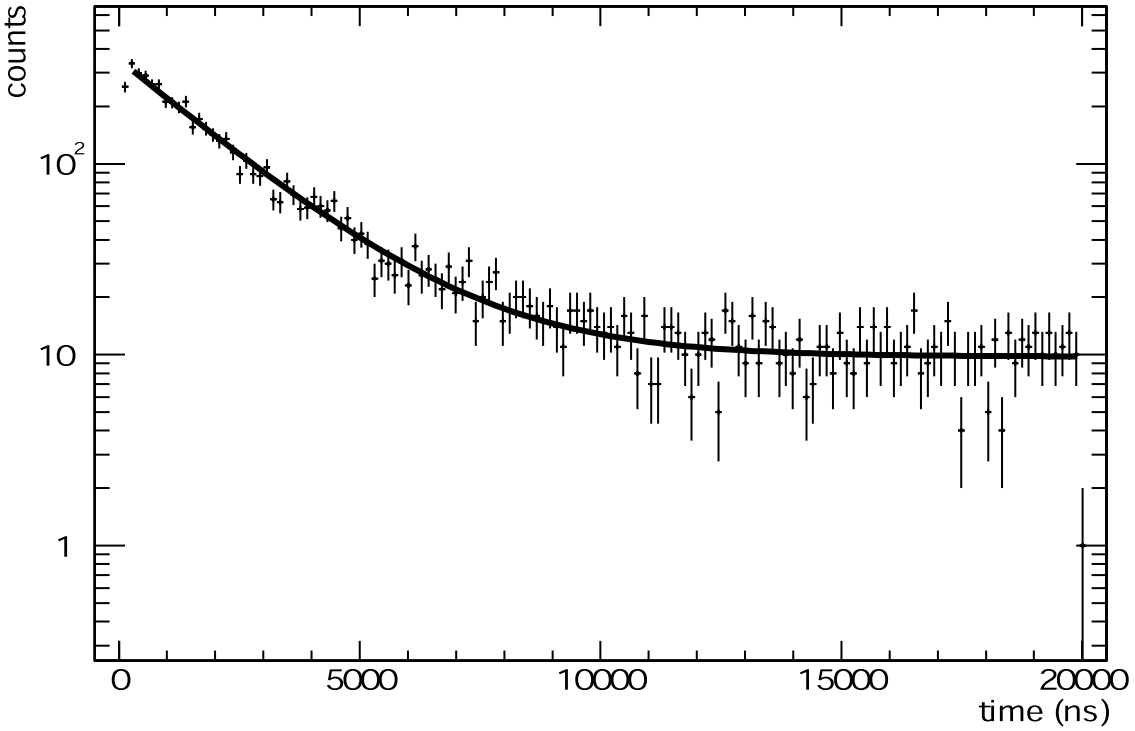

FIG. 10: Fitting the target-out data with Eqn. 22. Data includes 12735 up events, $\chi^2 = 1.02$.

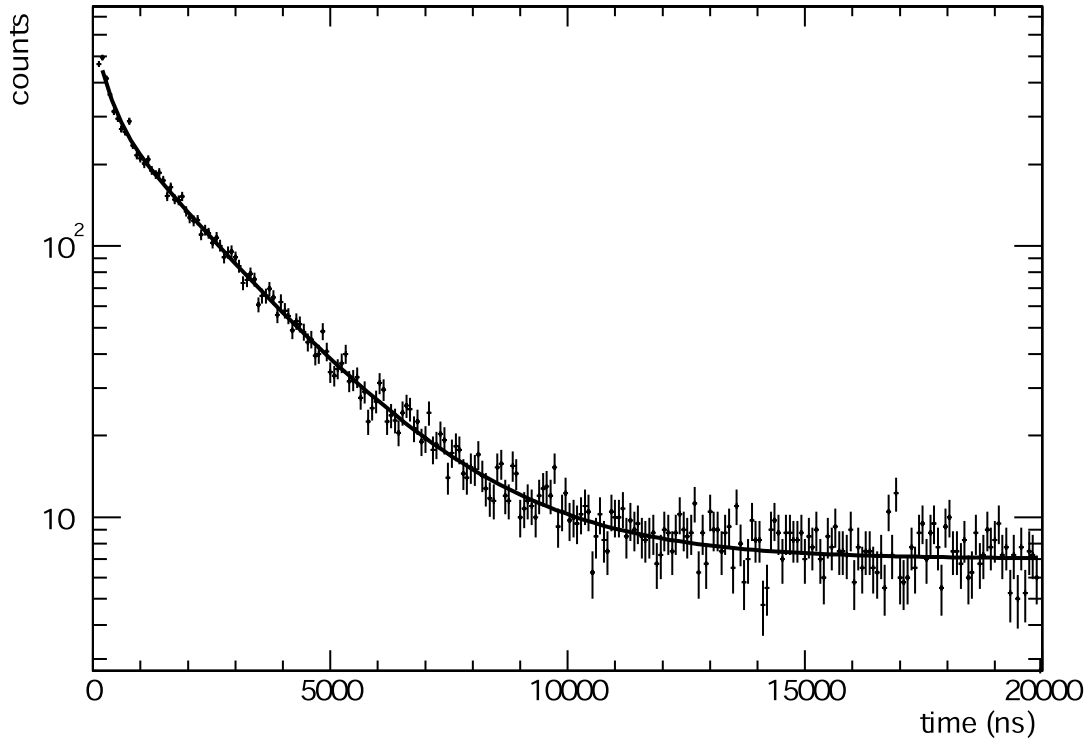

FIG. 11: Fitting the target-in data with Eqn. 23. Data includes 43674 events and the fit has $\chi^2 = 1.26$.

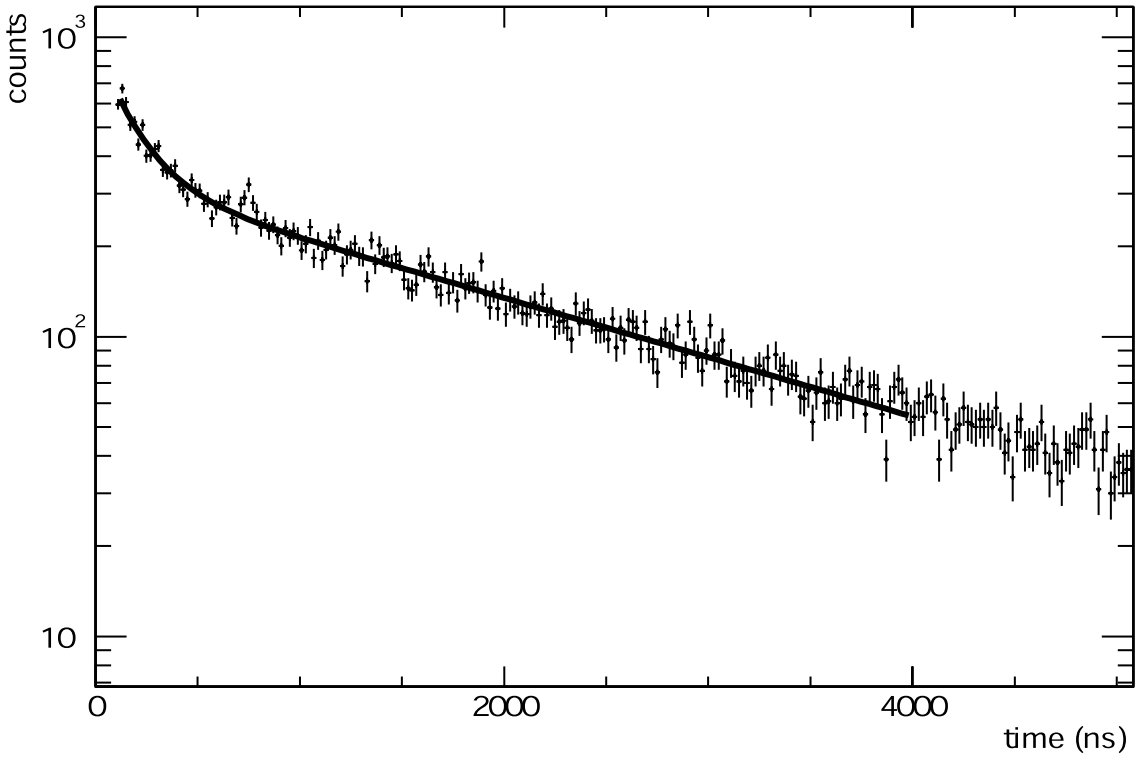

FIG. 12: Fitting the target-in data with Eqn. 23. This histogram is a blow-up of FIG. 11, with 20 ns bins in order to have better resolution on the μ^- lifetime in copper. Data includes 24048 events and the fit has $\chi^2 = 1.38$.

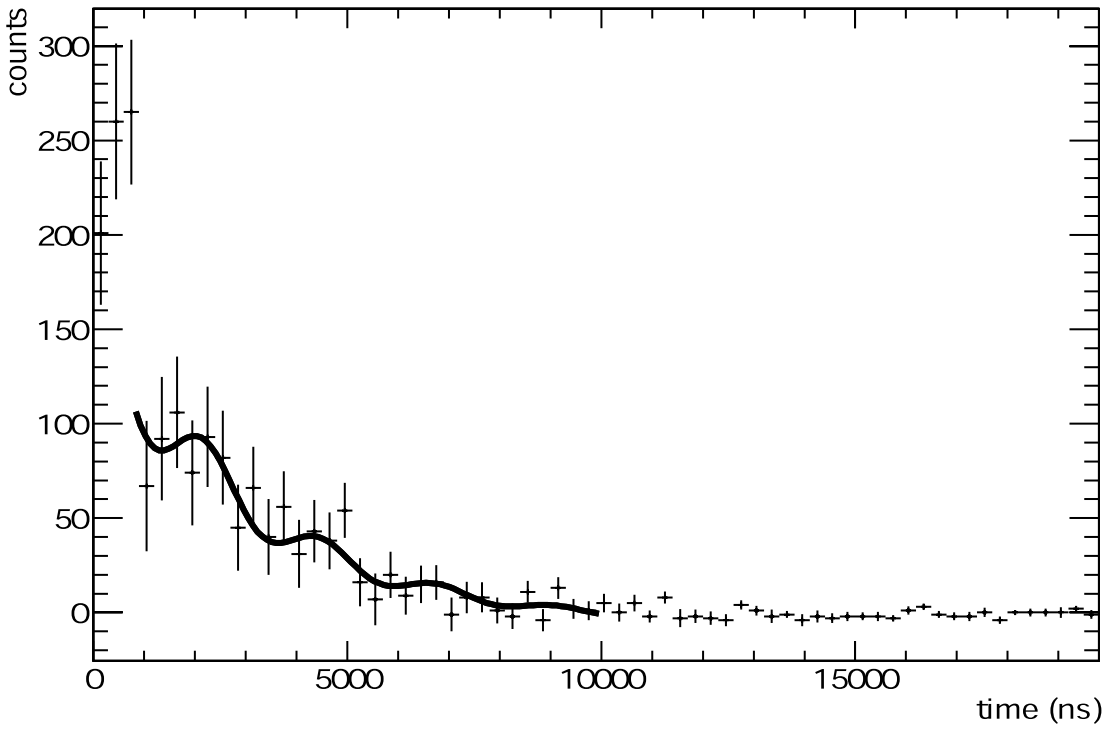

FIG. 13: Fitting the precession data with Eqn. 24. Data includes 14495 events and the fit has $\chi^2 = 1.09$.